Journal of Molecular Liquids 325 (2021) 115133

Contents lists available at ScienceDirect

Journal of Molecular Liquids

journal homepage: www.elsevier.com/locate/molliq

Carbon dioxide solubility in amine-based deep eutectic solvents: Experimental and theoretical investigation

Khatereh Ali Pishro, Ghulam Murshid *, Farouq Sabri Mjalli, Jamil Naser

Department of Petroleum & Chemical Engineering, Sultan Qaboos University, Muscat, Oman

ARTICLE INFO

Article history:
Received 13 October 2020
Received in revised form 16 December 2020
Accepted 18 December 2020
Available online 30 December 2020

Keywords:
Deep eutectic solvents
Ionic liquids
Carbon dioxide
Solubility
Henry constants
Modeling
Vapor-liquid equilibrium

ABSTRACT

In this work, ammonium-based Deep Eutectic Solvents (DES) were successfully synthesized using Ethanol amine hydrochloride, and tetraethylenepenta amine (EAHC-TEPA) as a hydrogen bond donor (HBD) with the molar ratios of 1:1, 1:3, 1:6, and 1:9. Carbon dioxide (CO_2) solubility was measured in the synthesized DESs above ratios at different pressures and temperatures. The molar ratio of 1:9 showed the best solubility for CO_2 among other ratios and was chosen for more in-depth investigation in this work. Solubility data was correlated using response surface methodology (RSM) and ANOVA analysis was performed. The results showed that the temperature and pressure have a significant effect on CO_2 solubility and a correlation was successfully developed. The FTIR, NMR characterization and Henry's constant along with other thermodynamic properties such as enthalpy and entropy of absorption were calculated. The physicochemical properties such as density, refractive index, and viscosity were also measured and correlated using a modified Graber and Vogel-Tamman-Fulcher (VTF) equations respectively.

1. Introduction

The increasing consumption of fossil fuels since the start of the industrial revolution has resulted in an ever-increasing demand for global energy. A significant amount of greenhouse gases (GHGs) were generated as a result of using fossil fuels in power plants, and other industries [53,83]. Global warming is now a phenomenon that causes wide concern and it is due to the release of carbon dioxide (CO_2), the major component of GHGs, into the atmosphere. The atmospheric CO_2 concentration increased to 400 ppm in 2019 as a direct result of industrial activity, and this has led to a 0.8 °C rise in the global temperature, [17,80]. Carbon emissions are expected to rise to 900 ppm by 2050 [17,80].

The CO_2 capture by using various processes is important to minimize its emissions in our environment and consequently enhances its significance in reducing global warming. Many methods have been developed in the past decades for capturing CO_2 including; amines and amino acids as solvents, membrane separation, cryogenic and adsorption [10,29,64,70,86]. Various solubility processes have been used to capture CO_2 due to the applicability of this process using different solvents [5]. Aqueous amines solvents such as; monoethanolamine (MEA), diethanolamine (DEA), and *n*-methyldiethanolamine (MDEA) have been used by industry for many years [26,34,47,59]. MEA has been reported as the most common solvent used to capture CO_2, but MEA has some drawbacks. It is corrosive, it has high volatility, a high regeneration temperature, and it is toxic [25].

Blended primary, secondary, and tertiary amines such as the combination of MEA or DEA with piperazine (PZ), 2-amino-2-methyl-1-propanol (AMP), and *n*-methyldiethanolamine (MDEA) were studied, as well [13,19,22,41,61]. None of these blends has attracted industrial attention, and further basic research is still required to develop new solvents for industrial application [72].

Recently, Ionic liquids (IL) received attention due to their ability to tune the solvents as per the required application. The ability to select anions and cations in ILs suggested they might be an attractive solvent for CO_2 capture [38,74]. However, the limitations associated with IL solvents, such as high viscosity after CO_2 solubility, high cost in bulk applications, toxicity, and biodegradability reduced the use of ILs in the industry [12,15,40]. Further global research is required to overcome the above weakness to make ILs a suitable choice for the industry.

However, most recently, a new class of ILs called Deep Eutectic Solvents (DESs) emerges as a potential alternate. These DESs are synthesized by the intermolecular attractions between the two components knowns as Hydrogen Bond Donors (HBDs) and Hydrogen Bond Acceptors (HBAs) [36]. These solvents have low melting points compared to ILs [67], moderating the ILs limitations for CO_2 capture through low operation costs, non-toxic and biodegradable materials [1].

Several studies of CO_2 solubility in different DESs have been reported in the literature [1,18,21,23,27,28,32,48,52,79].

* Corresponding author.
E-mail address: g.murshid@squ.edu.om (G. Murshid).

https://doi.org/10.1016/j.molliq.2020.115133
0167-7322/

Li et al. [52,] studied the CO_2solubilityin Choline Chloride based (ChCl:Urea) DES at various temperatures (313.15 K, 323.15 K, and 333.15 K) and up to 13 MPa pressure with different molar ratios (1:1.5, 1:2, and 1:2.5). It was found that all three variables; pressure, temperature and DES molar ratios affect the CO_2 solubility in the DES. The solubility of CO_2 in mixtures increased with increasing pressure and it was more sensitive to pressure in the low-pressure range. In another study [49,50] of CO_2 solubility in Choline chloride and ethylene glycol-based DESs, similar findings were reported. The solubility tends to increase with increasing pressure and decreases at higher temperatures.

[18] also reported the CO_2 solubility in ChCl-based DESs from a mixture with dihydric alcohols (1, 4-butanediol, 2, 3-butanediol, and 1, 2-propanediol) with a molar ratio of 1:3 and 1:4. DESs containing 2, 3-butanediol with a ratio of 1:4 showed the highest CO_2 solubility capacity. The solubility of CO_2 in the mixtures increased linearly with the increase of pressure or with decreasing temperature.

In addition to the above-mentioned literature, Amine based DESs are also emerging as an alternative potential solvents to capture CO_2 when compared to conventional aqueous alkanolamines or their blends [4]. When [37] used monoethanolamine (MEA) in aqueous ChCl/urea (choline chloride–urea (commercial name: reline) DES, CO_2 solubility increased by adding MEA. The measured solubility data was satisfactorily modeled by using the modified Kent–Eisenberg model.

In addition to the above-mentioned literature, [56] studied the solubility of carbon dioxide in monoethanolamine (MEA), diethanolamine (DEA), and *N*-methyldiethanolamine (N-MDEA) (30 wt%) when dissolved in a deep eutectic solvent of choline chloride and ethylene glycol at three different temperatures; 298.1, 313.1 and 333.1 K and pressure to 800 kPa, with on-line analysis of the gas phase using gas chromatography (GC). The results revealed that adding MEA and DEA, as opposed to adding N-MDEA to the DES, led to an increase in CO_2 capture. Their findings also revealed that the CO_2 solubility increased by increasing pressure and decreasing temperature. The literature consistently reports that amine-based DES is promising and needs more research.

Previously, [82] reported 33.7 wt% of CO_2 solubility in a novel DESs formed by monoethanolammonium chloride:ethylenediamine [MEA·Cl:EDA] or [EAHC:EDA] for the molar ratio of 1:3 at 303.15 K. The large CO_2 uptake in [MEA·Cl:EDA]based DESs was assumed to depend on the change in polarity and basicity [76] subsequently studied the CO_2 solubility of [MEA·Cl] DESs with more long-chain amines of HBDs such as; diethylenetriamine(DETA), tetraethylenepentamine (TEPA) pentaethylenehexamine (PEHA), 3-amino-1-propanol (AP), and aminomethoxypropanol (AMP).

To the best of our knowledge, previous studies on non-aqueous amine-based DESs, prepared by Ethanol amine hydrochloride; EAHC as HBA and TEPA as HBD are very limited. This fact prompted us to investigate these structures because they had produced very good results.

This study focused on the synthesis and characterization of amine-based DESs: EAHC:TEPA (1:9) to measure the solubility of CO_2 in synthesized DES under various operational conditions of pressure, ranging from 0.4 to 1.6 MPa, and a temperature range from 303.15 to 333.15 K, respectively. The experiments were designed using the Design of Experiment (DOE) statistical approach which is a well-known method used to evaluate the significance of each factor on the response and development of appropriate regression models. In much of the literature, DOE is used to study the effect of operating parameters and to find the optimal conditions [43,46,62,65,73,77]. Response surface methodology (RSM) can be employed as an effective technique of DOE fin developing, improving, and optimizing the significant factors in CO_2 capture. The formation of DES and reaction mechanism of EAHC:TEPA with CO_2 was successfully established using FT-IR and NMR spectroscopy. Henry's Law constant and other thermodynamic properties were also calculated.

Furthermore, the physical properties such as density, refractive index, and viscosity of the synthesized DESs (EAHC:TEPA) with ratios of 1:1, 1:3, 1:6, and 1:9 were measured at atmospheric pressure and temperature ranging from 298.15–333.15 K. The modified Graber model and modified Vogel-Tamman-Fulcher (VTF) equations were used for density, refractive index, and viscosity, respectively.

2. Material and methods

2.1. Chemicals and gases

Ethanolamine hydrochloride (EAHC) and Tetraethylenepentamine (TEPA) were purchased from Sigma-Aldrich. These chemicals were used without any further purification. Carbon dioxide gas (CO_2) with a purity of 99.999% and nitrogen gas (N_2) with a purity of 98% were used in this work which were sourced from a local supplier. The structure of the chemicals and their specifications are listed in Fig. S1 and Table S1 (supplementary material) respectively.

2.2. Preparation of the DESs

The DESs were prepared by EAHC:TEPA with molar ratios of 1:1,1:3, 1:6, and 1:9 using a magnetic stirrer equipped with a temperature control assembly. The mass of all the pure components was measured with a digital balance (Shimadzu, model AUW220D) with an accuracy of ± 0.1 mg. Each combination of EAHC and TEPA was mixed at 400 rpm for a minimum of 3 h at temperature up to 353.15 K. This stirring process continued until a homogeneous liquid was formed without any precipitation [2,27,39].

2.3. CO_2 solubility measurement

The solubility of CO_2 in EAHC:TEPA (1:9) solutions was measured using a high-pressure solubility cell as shown in Fig. S2. The solubility equipment was designed for a temperature range of 303.15 to 333.15 K and a pressure up to 20 bar. It includes two vessels; one is an equilibrium cell of 100 ml volume for CO_2 solubility and the other is a pressure vessel of 220 ml which is primarily used to generate the desired pressure. The electric heater containing two heating element was used to control the temperature of both cells with an accuracy of ±0.01 K. Both cells were purged with nitrogen before introducing any CO_2 into the system. CO_2 was then transferred directly from the cylinder and the desired pressure was maintained. The pressure of both vessels was measured with a digital pressure recorder (Crystal control, METEK, nVision) with an estimated accuracy of ±0.001 MPa. In each experiment, 6 ml of a non-aqueous sample was injected to Equilibrium Cell (EC). Then, CO_2 was introduced to the sample by transferring it from the Pressure Vessel (PV) at the specific pressure and temperature. A magnetic stirrer under the EC was turned on at 300 rpm to mix the purged CO_2 with the liquid inside the EC. The equilibrium time was attained after approximately 6–8 h when no further pressure drop was observed. The pressure gauge was connected to a computer to measure the pressure drop during the solubility until the equilibrium was reached. The pressure drop method had previously been adopted by other researchers in this field [25,27,35].

The moles of CO_2 transferred from the pressure vessel were calculated by the following equation; [2,5]

$$n_{CO2} = \frac{V_T}{RT_a}\left(\frac{P_1}{z_1} - \frac{P_2}{z_2}\right) \quad (1)$$

V_T is the volume of the gas container (pressure vessel), Z_1, and Z_2 are the compressibility factors for each pressure (P_1 and P_2), R is the gas constant and T_a is the ambient temperature. The equilibrium was achieved in 6–8 h. The equilibrium pressure (P_{CO2}) was recorded and the moles of CO_2 (in gas phase) were calculated by the following equation;

$$n^{g}_{CO_2} = \frac{V_g P_{CO_2}}{Z_{CO_2} RT} \quad (2)$$

V_g is the gas volume in the equilibrium cell and T is the operating temperature. The moles of CO_2 in the liquid phase and CO_2 solubility (α) were then calculated from the following equations respectively

$$n^{l}_{CO2} = n_{CO_2} - n^{g}_{CO2} \quad (3)$$

$$\alpha = \frac{n^{l}_{CO_2}}{n_{solvent}} \quad (4)$$

The experimental uncertainty of measured CO_2 solubility at a corresponding temperature was estimated to be as $\pm 4 \times 10^{-3}$ mol·mol^{-1} and $\pm$ 0.05 K, respectively.

2.4. FTIR analysis

The Infrared spectra of the DESs before and after CO_2 loading were obtained and compared in the range of 4000–650 cm^{-1} on a perkin-Elmer Spectrum 400 ATR-IR instrument (Waltham, MA) with an ATR force gauge (Shelton, CT).

2.5. Nuclear magnetic resonance(NMR) analysis

The NMR spectra of the studied DESs (before and after CO_2solubility) were obtained on AVANCE-III HD 700 MHz FT-NMR (Bruker Biospin). An AscendTM Superconducting Magnet System equipped with 3 channels and frequency range for each of 3 channels at 6–1020 MHz was used with TCI Triple Inverse Cryoprobe for 5 mm sample tubes. The homogenous samples of EAHC-TEPA before and after solubility of CO_2 transferred to the tubes, 5% distilled water also added to all samples for indicating the ingredients of the samples through H-NMR and C-NMR as required.

2.6. Density measurement

The densities of the synthesized DESs (EAHC:TEPA) with ratios of 1:1, 1:3, 1:6, and 1:9 were measured three times and only the average values were reported. All measurements were taken at atmospheric pressure and over a range of temperature from 298.15–333.15 K. The densities of DESs were measured using a density meter (A. KRUSS Optronic GmbH – DS7800) with a measuring accuracy of $\pm 1.0 \times 10^{-4}$ g·cm^{-3}, and a temperature-controlled accuracy of $\pm$0.01 K (PT 100). Before injecting the sample, the density meter was cleaned with ethanol and Millipore quality water.

2.7. Refractive index measurement

The refractive index of the non-aqueous prepared DES (EAHC:TEPA) with ratios of 1:1, 1:3, 1:6, and 1:9 was measured using a digital refractometer (RM 40, Mettler Toledo), with a measurement range of 1.3200 to 1.7000 n_D and measuring accuracy of $\pm$0.0001. The refracto meter was cleaned with both Millipore water and acetone to remove any residuals of the previous measurements. The built-in temperature control system that provided faster cooling and heating rates with a precision of $\pm$0.05 K.

2.8. Viscosity measurement

The viscosity of synthesized DESs with the same ratios as mentioned earlier at a temperature range of 29,815 to 333.15 K was measured using an Ubbelohde viscometer (Cannon-Fenske). The samples were immersed in a thermostatic bath (Tamson, TVB445) for at least 15 min with a temperature-controlled accuracy of 0.1 K. The efflux time was then measured using a stopwatch with an accuracy of 0.01 s and the viscosity values were reproducible within $\pm$1% of full scale.

The kinematic viscosity (η) was calculated by the following equation; Eq.

$$\eta = k.t \quad (5)$$

where k is the viscometer constant and t is the time measured in seconds. Each measurement was repeated three times and only the average values are reported.

2.9. Response surface methodology (RSM)

Design of Experiment (DOE) is an efficient way to plan experimental analysis and to yield valid and objective conclusions. The effects of temperature and pressure on the properties of prepared DES was studied using the DOE by selecting the user-defined option of response surface methodology (RSM). RSM is an important tool to evaluate the relative significance of factors helpful for modeling and optimizing processes. In this work, RSM was used to assess the effects of temperature and pressure on CO_2 solubility. The Quadratic regression model (Minitab and DOE expert) was developed to predict the CO_2 loading in the DES solutions. The interactions having a confidence interval level of over 99%, or a probability value less than 0.0001were considered to be highly significant responses.

3. Result and discussion

3.1. Calibration of equipment

To ensure the reliability and accuracy of the reported data, the density, viscosity and Reflective -index of known pure components already reported in the literature were measured and compared. This comparison was performed using the average absolute deviation (%AAD). This accuracy indicator is expressed in Eq. (6), and its value for the density, viscosity and Reflective-index calibration measurements is reported in Table 1.

$$\%AAD = \left(\frac{100}{N}\right) \sum_{i=1}^{N} \left| \frac{Y_i^{exp} - Y_i^{lit}}{Y_i^{exp}} \right| \quad (6)$$

where N is the number of experimental data points. The subscripts “exp” and ‘lit” represent the experimental and literature value of a quantity respectively. The lower computed values of %AADs given in Table 1 suggested the reliability and accuracy of the equipment used to investigate the physical properties data [68].

To calibrate the solubility measurement equipment, the solubility of CO_2 was measured in a 30 wt% Monoethanolamine (MEA) solution at 313.15 K and pressure of 0.5–2.4 MPa. The measured solubility vales obtained in this work along with the data obtained by [33,75] were also plotted and compared as shown in Fig. 1. Measured solubility values in this work showed a high level of agreement with the literature, with an average absolute deviation %AAD of 1.87 [75] and 1.7 [33].

3.2. CO_2 solubility

The Solubility of CO_2 in the prepared DES; EAHC:TEPA (1:9) was measured at different pressures and temperatures as mentioned earlier. This ratio was selected after screening since it has exhibited the highest CO_2 uptake value [71]. The solubility of other ratios of the synthesized DESs; EAHC:TEPA 1:1, 1:3, 1:6 and 1:9 were reported 0.272, 0.382, 0.594 and 0.702 at temperature 313.15 K and pressure 0.8 MPa, respectively. Since the DES with 1:9 showed higher affection for CO_2, therefore it was further studied for its characteristics toward CO_2 solubility. The experimental CO_2 solubility EAHC:TEPA (1,9) results are listed in Table 2 as a function of temperature and pressure. Solubility increased

Table 1
Comparison of experimental and literature data of density, viscosity and refractive Index.

ρ/(kgm^{-3})				η/(mPa.s)			*RI* (η_D)			
AHPD (20 *wt%*)[a]							Pure Water[b]			
Temp/(K)	Expt.	Lit.	%AAD	Expt.	Lit.	%AAD	Temp./(K)	Expt.	Lit.	%AAD
303.15	1.0475	1.0474		1.472	1.475		303.15	1.3319	1.33188	
313.15	1.0432	1.0434	0.012	1.169	1.17	0.13	313.15	1.3306	1.33053	0.0047
323.15	1.0391	1.039		0.963	0.962		323.15	1.3288	1.3289	
333.15	1.0331	1.033		0.783	0.782		333.15	1.3271	1.32704	

[a] Park et al. [68].
[b] Navarro et al. [66].

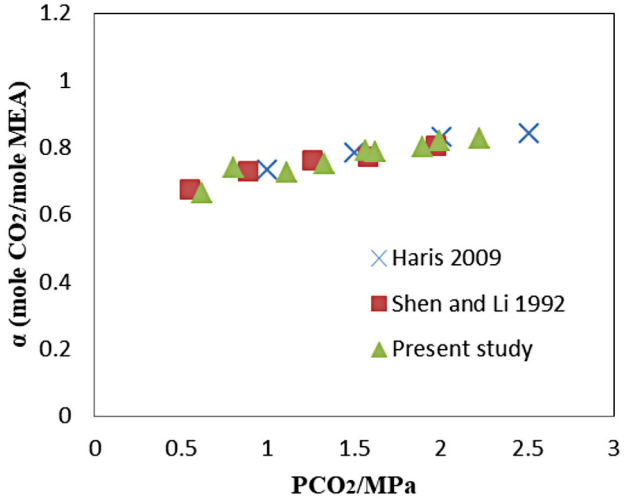

Fig. 1. Comparison of CO_2 solubility in 30 wt% aqueous MEA solutions at 313.15 K.

Table 2
CO_2 solubility data in non-aqueous DES; 1EAHC:9TEPA at temperatures 303.15, 313.15, 323.15 and 333.15 K.

T = 303.15 K		T = 313.15 K		T = 323.15 K		T = 333.15 K	
P_{CO2}/MPa	α_{CO2}	P_{CO2}/MPa	α_{CO2}	P_{CO2}/MPa	α_{CO2}	P_{CO2}/MPa	α_{CO2}
0.413	0.528	0.424	0.398	0.412	0.339	0.420	0.338
0.839	0.735	0.846	0.716	0.833	0.601	0.835	0.501
1.212	1.089	1.221	1.011	1.230	0.886	1.244	0.657
1.603	1.742	1.614	1.585	1.644	1.301	1.640	0.801

with the increase in CO_2 pressure, while it decreased with increasing the temperature. The solubility of CO_2 in previous studied DESs and ionic liquids at different pressures and temperatures reported similar trends [6,49,50,69]. The effects of temperature and pressure [7,49–51,78,85], have reported that by increasing temperature, the solubility of CO_2 in DES decreases. This could be due to the weakening of intermolecular interactions which lead to a higher rate of escape from the solution [7,8]. Similar findings were reported in other studies as choline chloride-based DESs investigated by [52,]revealed that the solubility of CO_2 in choline chloride and urea DESs depends upon pressure, temperature, and the DES ratio.

3.3. Regression analysis 1

In order to obtain predictive equations for CO_2solubility in DESs both linear and quadratic regression models were developed. The predictive equation was obtained by the regression model of α (CO_2 solubility) in relations of codded factors as following and the interaction parameters are presented in Table S2.

$$\alpha_{CO_2} = 0.8874 - 0.0899T + 0.2621P_{CO_2} - 0.0669TP_{CO_2} - 0.0319T^2 + 0.0225{P_{CO_2}}^2 - 0.0729T^2P_{CO_2} - 0.0493T{P_{CO_2}}^2 - 0.0018T^2 + 0.0400{*P_{CO2}}^2 \quad (7)$$

The model F-value of 433.44 implied that the model was significant [46].There was only a 0.01% chance that a large F-value could occur due to experimental noise. A *P*-value that was less than 0.05 indicated that model terms were significant. This model attained high accuracy value of more than 0.998 which indicated a good correlation with the experimental data. The percentage of coefficient variations (C·V) for 1EAHC:9TEPA system was 1.58 which means that the experiments were reliable as the CV values were so low. For the acceptability of the model, the optimum levels of operating parameters (pressure, temperature) were established and the absolute relative error (ARE) between the predicted and the experimental data was calculated.

$$ARE = \left| \frac{\text{Calculaed value} - \text{Predicted value}}{\text{calculated value}} \right| \quad (8)$$

ARE value smaller than 0.2 convinced the accuracy of statistical analyses, [87], and ARE value for $\alpha_{CO2}$of this work was 0.01989 which is within the acceptable range as reported. The ARE value indicated the consistency of the developed regression model for the prediction of CO_2 solubility.

The relationship between the calculated α_{CO2} and their predicted values were plotted as shown in Fig. S3. It was clear that the predicted α_{CO2} using the developed regression model was well in agreement with the calculated α_{CO2}value with an R^2 value of more than 0.99. In addition, Table S3 presents the experimental solubility data with the statistical model predictions, and standard deviation in non-aqueous DES; 1EAHC:9TEPA at temperatures of 303.15, 313.15, 323.15, 333.15 K.

Furthermore, Fig. S4. Shows a plot of the residuals versus the experimental run that was a method for testing model adequacy. It helps to identify any of the systematic error that could affect the response (α_{CO2}). Such a plot revealed that no systematic error was present in the background measurements.

To further analyze the influences of independent parameters on the response (α_{CO_2}), a three-dimensional (3-D) surface plot was created as shown in Fig. 2. It displays the three-dimensional representation of the measured solubility data along with the operating variables. Consequently, it demonstrates that a higher CO_2 loading would take place when pressure was higher and the temperature was adjusted at the lowest value of 303.15 K which is similar to earlier findings reported in the literature.

3.4. FTIR Spectroscopic Study of Species Distribution in EAHC-TEPA-CO_2

To investigate the interaction of the synthesized EAHC-TEPA with CO_2, FT-IR spectra of EAHC-TEPA were analyzed before and after CO_2 loading, and the result is presented in Fig. S5. The broadening of O–H stretching at 3500 and 2500 cm^{-1}, was indicted in the formation

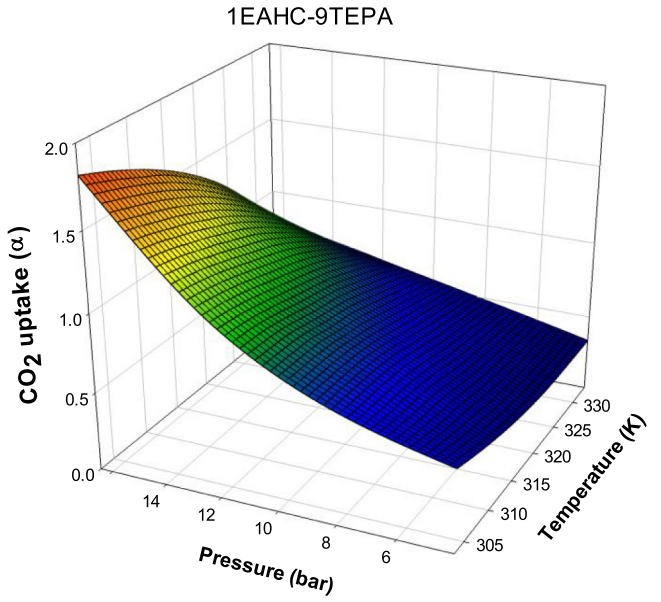

Fig. 2. Graphical representation of experimental CO_2 solubility data in terms of CO_2 loading.

of hydrogen bonds, and N–H bonding between EAHC and TEPA in EAHC-TEPA-CO_2.

The primary amine –N–H stretching peak at ~3300 $cm^{-1}$was reduced due to the formation of carbamate groups [31]. The absorption bands at ~1350-1500 cm^{-1} indicated the establishing of carbonate and bicarbonateCO_3^{2-}/HCO_3^-, and a strong peak at ~1600 cm^{-1}revealed the existence of CO_2 in the DES component [84].

3.5. NMR spectroscopic study of species distribution in EAHC-TEPA-H_2O–CO_2

The reaction mechanism and the binding of CO_2 with [EAHC][TEPA] has been described as the formation of carbamic acid upon reaction with CO_2 [44]. The carbamate anion ($RNHCOO^-$) was then formed due to the deprotonation of carbamic and protonation of amine forms $R'NH_3^+$.

NMR spectroscopy is the best-known method for studying chemical equilibrium in aqueous solutions. Many studies have been developed for quantitative NMR spectroscopy that allows the gaining of new insight in reacting multicomponent mixtures [57,58]. Through NMR spectroscopy, molecular structures can be distinguished even in similar components. Peak areas in NMR spectra directly reveal the molecular structure configuration of the components in the mixture [14,24,55].

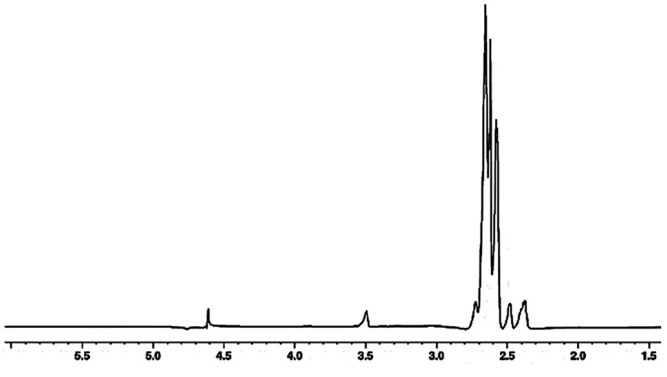

Fig. 3. ^1H NMR spectrum of EAHC-TEPA-H_2O before CO_2 adsorption at 298 K.

In the present work, NMR spectroscopy was used to determine the configuration of components in the prepared DESs; EAHC:TEPA: Water before and after CO_2 absorption. The chemistry configuration of the component was successfully detected as shown in Fig. 3 and Fig. S6-S8 (supplementary material), respectively.

Fig. 3 and Fig. S6. shows the ^1H NMR and ^{13}C NMR spectrum of EAHC-TEPA-Water, before the adsorption of CO_2 at 298 K while the Fig. S7, and Fig. S8 show the ^1H NMR and ^{13}C NMR spectrum of EAHC-TEPA-Water after the adsorption of CO_2 at 298 K. The reaction of an aqueous amine with bicarbonate results in the formation of the carbamate ($RNHCOO^-$) [11].

$$RNH_2 + HCO_3^- \rightarrow RNHCOO^- + H_2O \quad (9)$$

Similar studies have been reported by [79] with broadening of the NMR spectrum, and similar types of reactions were reported.

The main signals of different functional groups of molecules can be diagnosed by ^{13}C NMR and ^1H NMR spectra [16]. Presence of carbamate carbonyl (-CH_2-NH*COO*$^-$) at 164.3 ppm in ^{13}C NMR (Fig. S8) and the appearance of carbamate CH_2 (-CH_2-NHCOO$^-$) at 3.19 in ^1H NMR (Fig. S7) clearly indicates the adsorption of CO_2 in DES. The ^1H and ^{13}C NMR chemical shifts of important functional groups after the CO_2 adsorption are presented in the Table 3. The shifting of peaks are in accordance with the data reported earlier [44,76].

Fig. S9 illustrates the suggested intermolecular interaction of EAHC-TEPA-CO_2 by the NMR spectroscopic study of species distribution which revealed the formation of carbamate during the absorption of CO_2 through the solvent.

3.6. Henry's Law constant

Physical solubility of the gas in the solvents can be demonstrated by Henry's Law constant based on the mole fraction of the gas in the solvent (H_x) [69]. H_x quantitatively represents the solubility of CO_2 in the DESs through the following equation;

$$H_x(p,T) = \lim_{x_2 \to 0} \frac{f_2(p,T,x_2)}{x_2} \quad (10)$$

Where H_x is Henry's Law constant based on mole fraction, $f_2(p,T,x_2)$ is the fugacity of CO_2, p and x_2 are the partial pressure at the equilibrium state and the mole fraction of CO_2 in the liquid, respectively.

In a state of equilibrium, the fugacity of CO_2 in the liquid should be equal to that in the vapor phase. In this study, the vapor pressure of the DESs was very small at the experimental temperatures, and the gas phase, which was supposed to be pure CO_2, was approximately equal to unity.

Obviously, the fugacity coefficient of CO_2 at relatively low pressure could be calculated using a virial equation, and H_x can be expressed as following by the combination of equations;

$$H_x(p,T) = \lim_{x_2 \to 0} \frac{f_2(p,T,x_2)}{x_2} = \lim_{x_2 \to 0} \frac{p\Phi_2(p,T,y_2)}{x_2} \approx \frac{p\Phi_2(p,T)}{x_2} \quad (11)$$

Table 3
Typical NMR chemical shifts in EAHC-TEPA–H_2O–CO_2.

Detected Structure	Functional group	δ ^1H (ppm)	δ ^{13}C (ppm)
Carbonate/Bicarbonate	CO_3^{2-}/HCO_3^-	–	163.6
Carbonyl	–C–O–	–	–
Carbamate	-CH_2NH*COO*$^-$	–	164.3
	-*CH_2*NHCOO$^-$	3.19	43.4
Amine	*R*-NH_2	2.23, 2.43	46.8
Protonated Amine	*R*-NH_3^+	2.90	48.1
Carbamic acid	*R*NHCOOH	2.07	57.1
Hydroxymethylene	–*CH_2*-OH	3.0	60.9

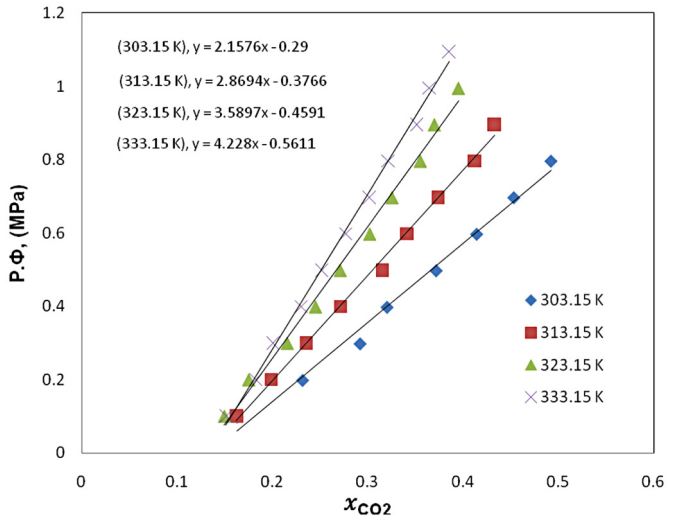

Fig. 4. Fugacity (P. Φ) vs. x_{CO2}(Mole Fraction) for the EAHC:TEPA(1:9) system different temperatures; 303.15 K, 313.15 K, 323.15 K, and 333.15 K.

Henry constant (H_x) at low pressures, is calculated through the linear slope of fugacity vs the mole fraction at different temperatures. The current results are plotted at different temperatures in Fig. 4 and are summarized in Table S4.

For further research, H_x at 313.15 K in this study was compared with those in other DESs and IL that were previously reported in the literature. As shown in Table 4, values of H_x in levuilinic acid:Chlorine-Chloride (3:1, 4:1, 5:1) and Furfuryl alcohol:Chlorine-Chloride (3:1, 4:1, 5:1) are much higher than those in the present study; EAHC:TEPA.

The values of H_x can be used to compare the CO_2 dissolution capacity of various solvents which are presented in Table 4. Since the Henry's constant data of amine based DESs are very limited and therefore the H_x data of the current work is compared with the data of other DES and ILs available in literature. The data in the Table 4 shows that the solubility of DES studied in the present work is higher than the other solvents (ILs and DESs) at the same temperature which is exhibited by lowest henry's constant value. These differences of the Henry constants reveal that long chain structure of TEPA in the synthesized DES (EAHC:TEPA) provides more active sites to absorb CO_2 [71].

To explore the strength of the interaction between carbon dioxide and the absorbent, the system enthalpy was calculated from Eq. (15). Meanwhile, the system entropy indicates the degree of order within the gas-liquid system which was calculated using Eq. (16) [9].

$$\Delta H = R\left(\frac{\delta \ln H_x}{\delta(1/T)}\right)_P \tag{12}$$

Table 4
Comparison of Henry constant of current study with other DESs and ILs at 313.15 K.

Solvent	H_x / MPa	Reference
levuilinic acid:Chlorine-Chloride (3:1)	21.91	[54]
levuilinic acid:Chlorine-Chloride (4:1)	20.39	[54]
levuilinic acid:Chlorine-Chloride (5:1)	20.12	[54]
Furfuryl alcohol:Chlorine-Chloride (3:1)	33.11	[54]
Furfuryl alcohol:Chlorine-Chloride (4:1)	29.95	[54]
Furfuryl alcohol:Chlorine-Chloride (5:1)	28.14	[54]
Hydroxyl Ammonium[hhemel]	25.6	[45,]
Hydroxyl Ammonium[hel]	16.5	[45,]
Choline Chloride (CH) + Urea(1:1.5)	18.5	[52,]
Choline Chloride (CH) + Urea(1:2)	12.3	[52,]
Choline Chloride (CH) + Urea(1:2.5)	22.4	[52,]
nCC:n1,4-butanediol (1:3)	43.66	[18]
EAHC:TEPA(1:9)	2.87	present study

$$\Delta S = -R\left(\frac{\delta \ln H_x}{\delta \ln T}\right)_P \tag{13}$$

Where ΔH and ΔS are the enthalpy and entropy of absorption, respectively. These two equations represent the slopes of Henry's constant data with temperature. The calculated value of the enthalpy of absorption is −18.856 kJ/mol whereas that for the entropy of absorption is −59.301 J/mol·K. The negative value of the enthalpy indicates a strong interaction between the carbon dioxide and the DES. Moreover, the negative value of the entropy is a sign of a high degree or order with the gas-liquid system. Compared to the industry standard CO_2 absorbent MEA 30 wt% which has a heat of absorption of −88.91 kmol [42], the DES has much less heat of absorption. This is a great advantage since this means that much less steam energy is needed to regenerate the solvent.

3.7. Physical properties measurements

In this work, the DES physical properties such as density, viscosity, and refractive index were measured as functions of DES various ratios (1:1, 1:3, 1:6 and 1:9) and temperature ranging from 298.15 K to 333.15 K.

Density is one of the physical characteristics that participates a crucial role in defining the performance of numerous manufacturing equipment, particularly those that are related to fluid dynamics and mass transfer. The experimental density of non-aqueous DESs; EAHC:TEPA with molar ratios of 1:1, 1:3, 1:6, and 1:9, and temperatures ranging from 298.15 to 333.15 K was investigated. The effect of molar ratio and temperature on density is presented in Fig. S10. The results show that the density decreases with an increase in temperature. This due to the expansion of the solution volume at higher temperatures, while the mass remains the same, which leads to a decrease in densities at relatively higher temperatures. On the other hand, at a given temperature, the density of the DESs of all systems decreased with the increase in their mole fraction of TEPA. By increasing the temperature from 298.15–333.15 K, density decreases linearly at all molar compositions of all studies DESs, because of the formation of larger intermolecular voids at high temperature, which increases the volume and subsequently decreases the density [60].

The refractive index is a dimensionless property that offers details about the optical characteristics of the liquid sample toward the light. It is used as an indirect quality indicator for the liquid. The measured refractive indices of the non-aqueous EAHC:TEPA solutions are given in Fig. S11. As shown in the figure, the variation trends of the refractive index were similar to that of densities with the temperature following the usual behavior observed for liquid systems. In general, the refractive index decreases with increasing temperature. This type of behavior is attributed to the impact of temperature on the kinetic energy and molecular movement patterns, which tends to cause the molecules to dislodge and boost the molar volume, and ultimately leads to a reduction of the refractive index value.

The viscosity of fluids is a very important physical property. It is used in the fluid flow design calculations and contributes to mass transfer and kinetic calculations. When liquids are mixed viscosity changes and consequently, this will affect the energy requirements in the design stage of equipment, pipes, and pumps. The experimental viscosities of non-aqueous system EAHC-TEPA were measured at different mole fractions and at temperatures ranging from 298.15 to 313.15 K.

The exponential decrease of viscosity with temperature is typical behavior for DES and ionic liquids as shown in Fig. S12. The change in fluid viscosity can be explained using the hole theory [3]. In this case the probability of finding suitable dimensional holes among the solvent molecules will increase with temperature increase due to the weakening of intermolecular forces [88]. Solvent molecules will have more opportunities to move through these holes and consequently the solvent fluidity will be enhanced. In addition, the change in DES composition

will alter the distribution of the intermolecular spaces within the fluid and consequently the viscosity decreases as TEPA concentration increases in the DES solution.

3.8. Modeling physical properties

It's very important to have accurate models that can predict physical properties data for the DES as a function of composition and temperature. The previously measured properties were modeled and validated using the experimental measurements.

To correlate the measured density data, modified Graber equation [30] was used since it can incorporate both variables (temperature and concentration) in one equation. The Graber model is considered as an inclusive model that can be used to predict the major physicochemical properties of binary mixtures which include temperature as a parameter. The general form of the Graber model is given in Eq. (14).

$$F(W,T) = W\ exp\left[A_1 + A_2T^{0.5} + A_3W^{0.5}\right] + A_4 \tag{14}$$

where F represents density or refractive index, W is the mass fraction of the corresponding component in the solution, T is the system's temperature and A_1 to A_4 are the empirical model parameters. To analyze the effect of both components (EAHC and TEPA) concentration on measured properties, Eq. (14) was amended into Eq. (15), as given below:

$$F(W_1,W_2,T) = (W_1+W_2)\ exp\left[A_1 + A_2T^{0.5} + A_3{W_1}^{0.5} + A_4{W_2}^{0.5}\right] + A_5 + A_6{W_1}^{0.5} + A_7{W_2}^{0.5} + A_8T^{0.5} \tag{15}$$

where W_1 and W_2 are the mass fractions of EAHC and TEPA respectively.

The root mean square error (RMSE) and the average absolute deviation (%ADD) were calculated according to the following equations:

$$\mathrm{RMSE} = \sqrt{\frac{\sum\left(Y_{exp} - Y_{pred}\right)^2}{n-k}} \tag{16}$$

$$\%AAD = \left(\frac{100}{N}\right)\sum_{i=1}^{i=n}\left|\frac{Y_{exp} - Y_{pred/lit}}{Y_{exp}}\right| \tag{17}$$

where Y_{exp} and $Y_{pred/lit}$ are experimental and predicted/literature data for the properties of binary mixtures, respectively; n is the number of experimental data and k is the number of the constant parameters of the model. The results of the density correlation are shown in Table S5.

Density values were fitted to the modified Graber equation by the method of least-squares using the Levenberg-Marquardt algorithm to estimate the corresponding parameters and the accuracy of the fit was evaluated by the root mean square error (RMSE) and coefficient of determination (R^2). Fig. 5. Presents the experimental density in comparison with calculated using Graber equation with R^2 value of 0.9916 which confirmed that the equation used is reliable for correlation of the density of the non-aqueous EAHC-TEPA binary mixture.

Refractive Index values were also fitted to Graber equation Eq. (15) using the same regression-based least-squares analysis. The calculated fitting parameters A_1-A_8 as well as the statistical indicators are given in Table S6.

The refractive index model validation is shown in Fig. 6. The coefficient of correlation (R^2) of 0.9916 confirmed that the equation used was reliable with a very narrow range of uncertainty.

The Vogel-Tamman-Fulcher (VTF) equation has been used in many studies [20,63,66,81] to correlate experimental viscosity data. The VTF equation is defined as follows:

$$\eta = \exp\left[V_0 + \frac{V_1}{T} + \frac{V_2}{T^2}\right] \tag{18}$$

In Eq. (18), η is the viscosity of DES EAHC:TEPA, T is the absolute temperature; and Vj ($j = 0, 1, 2$) are model parameters which were assumed to be dependent on the molar concentration of the solution. Such dependence was expressed in terms of a second-order polynomial as shown in Eq. (20)

$$V_j = v_{j,0} + v_{j,1}x + v_{j,2}x^2 \tag{19}$$

where $v_{j,0}$ to $v_{j,2}$ are the estimated fitting parameters investigated by correlating the experimental viscosity data using Eqs. (18) and (19) to find the minimum value of the objective function (%AAD). Nevertheless, an alternative form (Eq. (20)) was used in the work which involves the effect of concentration of the DES components on viscosity predictions.

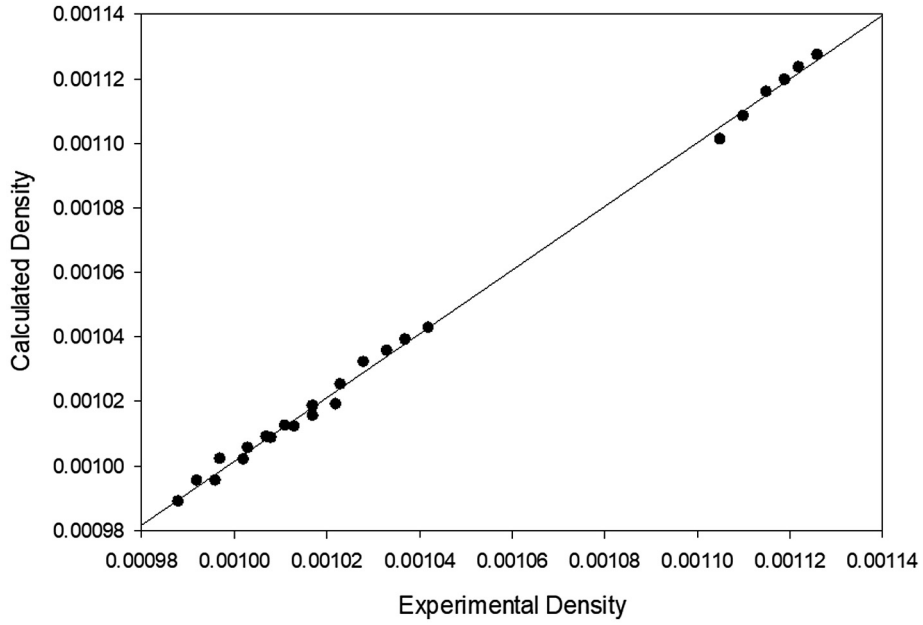

Fig. 5. Experimental and calculated density data of the non-aqueous system of EAHC-TEPA using a modified Graber equation.

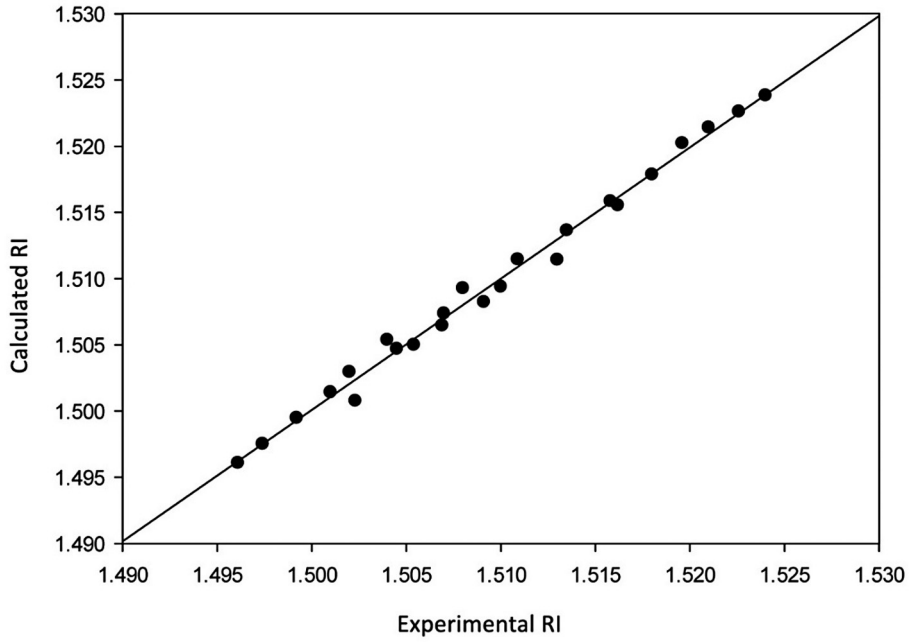

Fig. 6. Experimental and calculated refractive index data of the non-aqueous system of EAHC-TEPA using a modified Graber equation.

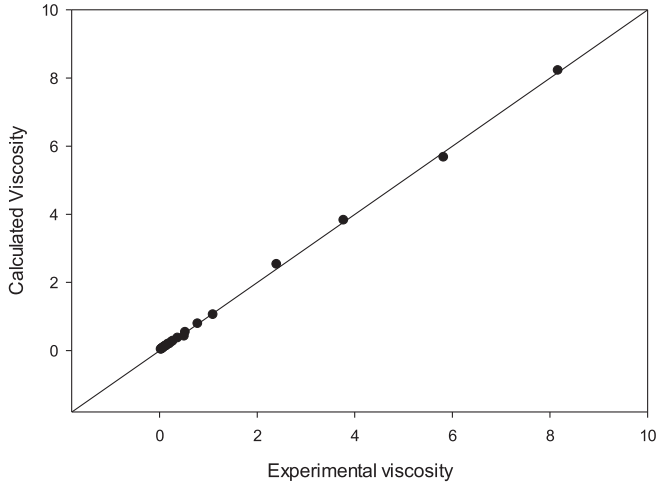

Fig. 7. Plot of experimental and calculated viscosity for different mole fraction of non-aqueous solution EAHC:TEPA.

$$V_j = v_{j,0} + v_{j,1}x_1 + v_{j,2}x_2 \quad (20)$$

Where $x_1$and$x_2$are the molar fractions of the salt and TEPA respectively, and $v_{j,0}$ to $v_{j,2}$ are optimized fitting parameters presented in Table S7 along with the minimized value of the objective function (% AAD). The measured and predicted data is represented in Fig. 7 and R^2 value (0.9994) indicates that there is a good agreement between correlated and experimental data.

4. Conclusion

The objective of this study was to determine the effectiveness of newly synthesize DES based on the EAHC salt and TEPA as the hydrogen bond donor for CO_2 solubility. The CO_2 solubility of the synthesized DESs at different pressures and temperatures was determined experimentally by the pressure drop method and then correlated successfully by the response surface methodology (RSM). The synthesis of DES and its reaction with CO_2 was studied using FTIR and NMR spectroscopy.

The CO_2 solubility was expressed in terms of the Henry's constant and the low value of the Henry's constant (EAHC:TEPA) compare to other DES and ILs shows that the presented DES in this study has better CO_2 dissolution capacity. In addition the enthalpy and entropy of absorption were also calculated. The important physical properties such as density, viscosity and refractive index were measured and correlated as a function of both temperature and DES composition. The new DES show competing performance compare to other DES and ILs. In addition to their known merits of the eutectic solvents, suggests that this can be a promising alternative to the traditional amine solvents.

Author statement

We are pleased to submit the above said manuscript titled “Carbon dioxide solubility in amine-based deep eutectic solvents: Experimental and theoretical investigation” in your esteemed journal. This manuscript has not been submitted to, nor is under review at, another journal or other publishing venue.

Declaration of Competing Interest

None.

Acknowledgements

We would like to thank and acknowledge Sultan Qaboos University, Oman for providing all the financial and technical support to complete this work.

Appendix A. Supplementary data

Supplementary data to this article can be found online at https://doi.org/10.1016/j.molliq.2020.115133.

References

[1] A.P. Abbott, D. Boothby, G. Capper, D.L. Davies, R.K. Rasheed, Deep eutectic solvents formed between choline chloride and carboxylic acids: versatile alternatives to ionic liquids, J. Am. Chem. Soc. 126 (29) (2004) 9142–9147.

[2] A.P. Abbott, G. Capper, D.L. Davies, R.K. Rasheed, V. Tambyrajah, Novel solvent properties of choline chloride/urea mixtures, Chem. Commun. 1 (2003) 70–71.

[3] A.P. Abbott, G. Capper, S. Gray, Design of improved deep eutectic solvents using hole theory, ChemPhysChem 7 (4) (2006) 803–806.

[4] I. Adeyemi, M.R. Abu-Zahra, I. Alnashef, Experimental study of the solubility of CO2 in novel amine based deep eutectic solvents, Energy Procedia 105 (2017) 1394–1400.

[5] A. Aftab, A. Shariff, S. Garg, B. Lal, M. Shaikh, N. Faiqa, Solubility of CO2 in aqueous sodium β-alaninate: experimental study and modeling using Kent Eisenberg model, Chem. Eng. Res. Des. 131 (2018) 385–392.

[6] S.N. Aki, B.R. Mellein, E.M. Saurer, J.F. Brennecke, High-pressure phase behavior of carbon dioxide with imidazolium-based ionic liquids, J. Phys. Chem. B 108 (52) (2004) 20355–20365.

[7] E. Ali, M.K. Hadj-Kali, S. Mulyono, I. Alnashef, A. Fakeeha, F. Mjalli, A. Hayyan, Solubility of CO2 in deep eutectic solvents: experiments and modelling using the Peng–Robinson equation of state, Chem. Eng. Res. Des. 92 (10) (2014) 1898–1906.

[8] T. Altamash, M.S. Nasser, Y. Elhamarnah, M. Magzoub, R. Ullah, H. Qiblawey, S. Aparicio, M. Atilhan, Gas solubility and rheological behavior study of betaine and alanine based natural deep eutectic solvents (NADES), J. Mol. Liq. 256 (2018) 286–295.

[9] J.L. Anthony, J.L. Anderson, E.J. Maginn, J.F. Brennecke, Anion effects on gas solubility in ionic liquids, J. Phys. Chem. B 109 (13) (2005) 6366–6374.

[10] A. Aroonwilas, A. Chakma, P. Tontiwachwuthikul, A. Veawab, Mathematical modelling of mass-transfer and hydrodynamics in CO2 absorbers packed with structured packings, Chem. Eng. Sci. 58 (17) (2003) 4037–4053.

[11] M.K. Aroua, A. Benamor, M.Z. Haji-Sulaiman, Equilibrium constant for carbamate formation from monoethanolamine and its relationship with temperature, J. Chem. Eng. Data 44 (5) (1999) 887–891.

[12] R.J. Bernot, E.E. Kennedy, G.A. Lamberti, Effects of ionic liquids on the survival, movement, and feeding behavior of the freshwater snail, Physa acuta, Environ. Toxicol. Chem. 24 (7) (2005) 1759–1765.

[13] S. Bishnoi, G.T. Rochelle, Absorption of carbon dioxide into aqueous piperazine: reaction kinetics, mass transfer and solubility, Chem. Eng. Sci. 55 (22) (2000) 5531–5543.

[14] S. Bishnoi, G.T. Rochelle, Thermodynamics of piperazine/methyldiethanolamine/water/carbon dioxide, Ind. Eng. Chem. Res. 41 (3) (2002) 604–612.

[15] L.A. Blanchard, D. Hancu, E.J. Beckman, J.F. Brennecke, Green processing using ionic liquids and CO 2, Nature 399 (6731) (1999) 28–29.

[16] W. Böttinger, M. Maiwald, H. Hasse, Online NMR spectroscopic study of species distribution in MDEA− H2O− CO2 and MDEA− PIP− H2O− CO2, Ind. Eng. Chem. Res. 47 (20) (2008) 7917–7926.

[17] I.C. Change, Mitigation of Climate Change. Contribution of WORKING GROUP III to the Fifth Assessment rePort of the Intergovernmental Panel on Climate Change, United Kingdom and New York, USA, Cambridge, 2014.

[18] Y. Chen, N. Ai, G. Li, H. Shan, Y. Cui, D. Deng, Solubilities of carbon dioxide in eutectic mixtures of choline chloride and dihydric alcohols, J. Chem. Eng. Data 59 (4) (2014) 1247–1253.

[19] W.-J. Choi, K.-C. Cho, S.-S. Lee, J.-G. Shim, H.-R. Hwang, S.-W. Park, K.-J. Oh, Removal of carbon dioxide by absorption into blended amines: kinetics of absorption into aqueous AMP/HMDA, AMP/MDEA, and AMP/piperazine solutions, Green Chem. 9 (6) (2007) 594–598.

[20] F. Civan, Brine viscosity correlation with temperature using the Vogel-Tammann-Fulcher (VTF) equation, SPE Drill. Complet. 22 (04) (2007) 341–355.

[21] G. Cui, M. Lv, D. Yang, Efficient CO 2 absorption by azolide-based deep eutectic solvents, Chem. Commun. 55 (10) (2019) 1426–1429.

[22] O.F. Dawodu, A. Meisen, Degradation of alkanolamine blends by carbon dioxide, Can. J. Chem. Eng. 74 (6) (1996) 960–966.

[23] D. Deng, Y. Jiang, X. Liu, Z. Zhang, N. Ai, Investigation of solubilities of carbon dioxide in five levulinic acid-based deep eutectic solvents and their thermodynamic properties, J. Chem. Thermodyn. 103 (2016) 212–217.

[24] V. Ermatchkov, Á.P.-S. Kamps, G. Maurer, Chemical equilibrium constants for the formation of carbamates in (carbon dioxide+ piperazine+ water) from 1H-NMR-spectroscopy, J. Chem. Thermodyn. 35 (8) (2003) 1277–1289.

[25] S. Garg, A. Shariff, M. Shaikh, B. Lal, A. Aftab, N. Faiqa, VLE of CO2 in aqueous potassium salt of L-phenylalanine: experimental data and modeling using modified Kent-Eisenberg model, J. Nat. Gas Sci. Eng. 34 (2016) 864–872.

[26] S. Garg, A. Shariff, M. Shaikh, B. Lal, H. Suleman, N. Faiqa, Experimental data, thermodynamic and neural network modeling of CO2 solubility in aqueous sodium salt of l-phenylalanine, J. CO2 Utiliz. 19 (2017) 146–156.

[27] H. Ghaedi, M. Ayoub, S. Sufian, A.M. Shariff, S.M. Hailegiorgis, S.N. Khan, CO2 capture with the help of Phosphonium-based deep eutectic solvents, J. Mol. Liq. 243 (2017) 564–571.

[28] H. Ghaedi, M. Ayoub, S. Sufian, A.M. Shariff, B. Lal, C.D. Wilfred, Density and refractive index measurements of transition-temperature mixture (deep eutectic analogues) based on potassium carbonate with dual hydrogen bond donors for CO2 capture, J. Chem. Thermodyn. 118 (2018) 147–158.

[29] M. Ghulam, S.A. Mohd, B.M. Azmi, Solubility of carbon dioxide in aqueous solution of 2-amino-2-hydroxymethyl-1, 3-propanediol at elevated pressures, Res. J. Chem. Env. 17 (2013) 41–45.

[30] T.A. Graber, H.R. Galleguillos, C. Céspedes, M.E. Taboada, Density, refractive index, viscosity, and electrical conductivity in the Na2CO3+ poly (ethylene glycol)+ H2O system from (293.15 to 308.15) K, J. Chem. Eng. Data 49 (5) (2004) 1254–1257.

[31] B.E. Gurkan, J.C. de la Fuente, E.M. Mindrup, L.E. Ficke, B.F. Goodrich, E.A. Price, W.F. Schneider, J.F. Brennecke, Equimolar CO2 absorption by anion-functionalized ionic liquids, J. Am. Chem. Soc. 132 (7) (2010) 2116–2117.

[32] M.C. Gutiérrez, D. Carriazo, C.O. Ania, J.B. Parra, M.L. Ferrer, F. del Monte, Deep eutectic solvents as both precursors and structure directing agents in the synthesis of nitrogen doped hierarchical carbons highly suitable for CO 2 capture, Energy Environ. Sci. 4 (9) (2011) 3535–3544.

[33] F. Harris, K.A. Kurnia, M.I.A. Mutalib, M. Thanapalan, Solubilities of carbon dioxide and densities of aqueous sodium glycinate solutions before and after CO2 absorption, J. Chem. Eng. Data 54 (1) (2008) 144–147.

[34] R.J. Hook, An investigation of some sterically hindered amines as potential carbon dioxide scrubbing compounds, Ind. Eng. Chem. Res. 36 (5) (1997) 1779–1790.

[35] M. Hosseini Jenab, M. Abedinzadegan Abdi, S.H. Najibi, M. Vahidi, N.S. Matin, Solubility of carbon dioxide in aqueous mixtures of N-methyldiethanolamine+ piperazine + sulfolane, J. Chem. Eng. Data 50 (2) (2005) 583–586.

[36] Y. Hou, Y. Gu, S. Zhang, F. Yang, H. Ding, Y. Shan, Novel binary eutectic mixtures based on imidazole, J. Mol. Liq. 143 (2–3) (2008) 154–159.

[37] Y.-H. Hsu, R.B. Leron, M.-H. Li, Solubility of carbon dioxide in aqueous mixtures of (reline+ monoethanolamine) at T=(313.2 to 353.2) K, J. Chem. Thermodyn. 72 (2014) 94–99.

[38] J. Huang, T. Rüther, Why are ionic liquids attractive for CO2 absorption? An overview, Aust. J. Chem. 62 (4) (2009) 298–308.

[39] B. Jibril, F. Mjalli, J. Naser, Z. Gano, New tetrapropylammonium bromide-based deep eutectic solvents: synthesis and characterizations, J. Mol. Liq. 199 (2014) 462–469.

[40] M.A. Kareem, F.S. Mjalli, M.A. Hashim, I.M. AlNashef, Phosphonium-based ionic liquids analogues and their physical properties, J. Chem. Eng. Data 55 (11) (2010) 4632–4637.

[41] S.N. Khan, S.M. Hailegiorgis, Z. Man, S. Garg, A.M. Shariff, S. Farrukh, M. Ayoub, H. Ghaedi, High-pressure absorption study of CO2 in aqueous N-methyldiethanolamine (MDEA) and MDEA-piperazine (PZ)-1-butyl-3-methylimidazolium trifluoromethanesulfonate [bmim][OTf] hybrid solvents, J. Mol. Liq. 249 (2018) 1236–1244.

[42] Y.E. Kim, J.A. Lim, S. Jeong, Y. Yoon, S.T. Bae, S.C. Nam, Comparison of carbon dioxide absorption in aqueous MEA, DEA, TEA, and AMP solutions, 34 (2013) 783–787.

[43] M. Kincl, S. Turk, F. Vrečer, Application of experimental design methodology in development and optimization of drug release method, Int. J. Pharm. 291 (1–2) (2005) 39–49.

[44] J. Kothandaraman, A. Goeppert, M. Czaun, G.A. Olah, G.S. Prakash, CO 2 capture by amines in aqueous media and its subsequent conversion to formate with reusable ruthenium and iron catalysts, Green Chem. 18 (21) (2016) 5831–5838.

[45] K. Kurnia, F. Harris, C. Wilfred, M.A. Mutalib, T. Murugesan, Thermodynamic properties of CO2 absorption in hydroxyl ammonium ionic liquids at pressures of (100–1600) kPa, J. Chem. Thermodyn. 41 (10) (2009) 1069–1073.

[46] Z.R. Lazic, Design of Experiments in Chemical Engineering: A Practical Guide, John Wiley & Sons, 2006.

[47] D. Le Tourneux, I. Iliuta, M.C. Iliuta, S. Fradette, F. Larachi, Solubility of carbon dioxide in aqueous solutions of 2-amino-2-hydroxymethyl-1, 3-propanediol, Fluid Phase Equilib. 268 (1–2) (2008) 121–129.

[48] R.B. Leron, A. Caparanga, M.-H. Li, Carbon dioxide solubility in a deep eutectic solvent based on choline chloride and urea at T= 303.15–343.15 K and moderate pressures, J. Taiwan Inst. Chem. Eng. 44 (6) (2013) 879–885.

[49] R.B. Leron, M.-H. Li, Solubility of carbon dioxide in a choline chloride–ethylene glycol based deep eutectic solvent, Thermochim. Acta 551 (2013) 14–19.

[50] R.B. Leron, M.-H. Li, Solubility of carbon dioxide in a eutectic mixture of choline chloride and glycerol at moderate pressures, J. Chem. Thermodyn. 57 (2013) 131–136.

[51] G. Li, D. Deng, Y. Chen, H. Shan, N. Ai, Solubilities and thermodynamic properties of CO2 in choline-chloride based deep eutectic solvents, J. Chem. Thermodyn. 75 (2014) 58–62.

[52] X. Li, M. Hou, B. Han, X. Wang, L. Zou, Solubility of CO2 in a choline chloride + urea eutectic mixture, J. Chem. Eng. Data 53 (2) (2008) 548–550.

[53] J.-A. Lim, D.H. Kim, Y. Yoon, S.K. Jeong, K.T. Park, S.C. Nam, Absorption of CO2 into aqueous potassium salt solutions of L-alanine and L-proline, Energy Fuel 26 (6) (2012) 3910–3918.

[54] M. Lu, G. Han, Y. Jiang, X. Zhang, D. Deng, N. Ai, Solubilities of carbon dioxide in the eutectic mixture of levulinic acid (or furfuryl alcohol) and choline chloride, J. Chem. Thermodyn. 88 (2015) 72–77.

[55] R.N. Maddox, G.J. Mains, M.A. Rahman, Reactions of carbon dioxide and hydrogen sulfide with some alkanolamines, Ind. Eng. Chem. Res. 26 (1) (1987) 27–31.

[56] M.-R. Mahi, I. Mokbel, L. Negadi, F. Dergal, J. Jose, Experimental solubility of carbon dioxide in monoethanolamine, or diethanolamine or N-methyldiethanolamine (30 wt%) dissolved in deep eutectic solvent (choline chloride and ethylene glycol solution), J. Mol. Liq. 289 (2019) 111062.

[57] M. Maiwald, H.H. Fischer, Y.-K. Kim, K. Albert, H. Hasse, Quantitative high-resolution on-line NMR spectroscopy in reaction and process monitoring, J. Magn. Reson. 166 (2) (2004) 135–146.

[58] M. Maiwald, H.H. Fischer, Y.-K. Kim, H. Hasse, Quantitative on-line high-resolution NMR spectroscopy in process engineering applications, Anal. Bioanal. Chem. 375 (8) (2003) 1111–1115.

[59] B. Mandal, M. Guha, A. Biswas, S. Bandyopadhyay, Removal of carbon dioxide by absorption in mixed amines: modelling of absorption in aqueous MDEA/MEA and AMP/MEA solutions, Chem. Eng. Sci. 56 (21−22) (2001) 6217–6224.

[60] F.S. Mjalli, G. Murshid, S. Al-Zakwani, A. Hayyan, Monoethanolamine-based deep eutectic solvents, their synthesis and characterization, Fluid Phase Equilib. 448 (2017) 30–40.

[61] M.K. Mondal, Solubility of carbon dioxide in an aqueous blend of diethanolamine and piperazine, J. Chem. Eng. Data 54 (9) (2009) 2381–2385.
[62] D.C. Montgomery, Design and Analysis of Experiments, John wiley & sons, 2017.
[63] G. Murshid, H. Ghaedi, M. Ayoub, S. Garg, W. Ahmad, Experimental and correlation of viscosity and refractive index of non-aqueous system of diethanolamine (DEA) and dimethylformamide (DMF) for CO2 capture, J. Mol. Liq. 250 (2018) 162–170.
[64] G. Murshid, F.S. Mjalli, J. Naser, S. Al-Zakwani, A. Hayyan, Novel diethanolamine based deep eutectic mixtures for carbon dioxide (CO2) capture: synthesis and characterisation, Phys. Chem. Liq. 57 (4) (2019) 473–490.
[65] R.H. Myers, D.C. Montgomery, Response Surface Methodology: Process and Product Optimization Using Designed Experiments, York, Wiley New, 1995.
[66] S.S. Navarro, R.B. Leron, A.N. Soriano, M.-H. Li, Thermophysical property characterization of aqueous amino acid salt solution containing serine, J. Chem. Thermodyn. 78 (2014) 23–31.
[67] C.A. Nkuku, R.J. LeSuer, Electrochemistry in deep eutectic solvents, J. Phys. Chem. B 111 (46) (2007) 13271–13277.
[68] J.-Y. Park, S.J. Yoon, H. Lee, J.-H. Yoon, J.-G. Shim, J.K. Lee, B.-Y. Min, H.-M. Eum, Density, viscosity, and solubility of CO2 in aqueous solutions of 2-Amino-2-hydroxymethyl-1, 3-propanediol, J. Chem. Eng. Data 47 (4) (2002) 970–973.
[69] A. Perez-Salado Kamps, D. Tuma, J. Xia, G. Maurer, Solubility of CO2 in the ionic liquid [bmim][PF6], J. Chem. Eng. Data 48 (3) (2003) 746–749.
[70] J. Pires, F. Martins, M. Alvim-Ferraz, M. Simões, Recent developments on carbon capture and storage: an overview, Chem. Eng. Res. Des. 89 (9) (2011) 1446–1460.
[71] K.A. Pishro, G. Murshid, F.S. Mjalli, J. Naser, Investigation of CO2 solubility in monoethanolamine hydrochloride based deep eutectic solvents and physical properties measurements, Chin. J. Chem. Eng. 28 (11) (2020) 2848–2856.
[72] L. Raynal, P.-A. Bouillon, A. Gomez, P. Broutin, From MEA to demixing solvents and future steps, a roadmap for lowering the cost of post-combustion carbon capture, Chem. Eng. J. 171 (3) (2011) 742–752.
[73] S. Sadeghi, M.R. Alavi Moghaddam, M. Arami, Techno-economical evaluation of hexavalent chromium removal by electrocoagulation process with the aid of polyaluminum chloride as coagulant: optimization through response surface methodology, Environ. Eng. Manag. J. 16 (1) (2017).
[74] L.G. Sánchez, G. Meindersma, A. De Haan, Solvent properties of functionalized ionic liquids for CO2 absorption, Chem. Eng. Res. Des. 85 (1) (2007) 31–39.
[75] K.P. Shen, M.H. Li, Solubility of carbon dioxide in aqueous mixtures of monoethanolamine with methyldiethanolamine, J. Chem. Eng. Data 37 (1) (1992) 96–100.
[76] S.K. Shukla, J.-P. Mikkola, Intermolecular interactions upon carbon dioxide capture in deep-eutectic solvents, Phys. Chem. Chem. Phys. 20 (38) (2018) 24591–24601.
[77] G.S. Simate, S. Ndlovu, M. Gericke, Bacterial leaching of nickel laterites using chemolithotrophic microorganisms: process optimisation using response surface methodology and central composite rotatable design, Hydrometallurgy 98 (3–4) (2009) 241–246.
[78] A.N. Soriano, B.T. Doma Jr., M.-H. Li, Solubility of carbon dioxide in 1-ethyl-3-methylimidazolium tetrafluoroborate, J. Chem. Eng. Data 53 (11) (2008) 2550–2555.
[79] L.L. Sze, S. Pandey, S. Ravula, S. Pandey, H. Zhao, G.A. Baker, S.N. Baker, Ternary deep eutectic solvents tasked for carbon dioxide capture, ACS Sustain. Chem. Eng. 2 (9) (2014) 2117–2123.
[80] P. Tans, R. Keeling, Trends in atmospheric carbon dioxide, NOAA/ESRL (www. esrl. noaa. gov/gmd/ccgg/trends/). Scripps Institution of Oceanography (scrippsco2. ucsd. edu/), 2014 , Last assessed on **17**.
[81] L.-A. Tirona, R.B. Leron, A.N. Soriano, M.-H. Li, Densities, viscosities, refractive indices, and electrical conductivities of aqueous alkali salts of α-alanine, J. Chem. Thermodyn. 77 (2014) 116–122.
[82] T.J. Trivedi, J.H. Lee, H.J. Lee, Y.K. Jeong, J.W. Choi, Deep eutectic solvents as attractive media for CO 2 capture, Green Chem. 18 (9) (2016) 2834–2842.
[83] J. van Holst, G. Versteeg, D.W.F. Brilman, J. Hogendoorn, Kinetic study of CO2 with various amino acid salts in aqueous solution, Chem. Eng. Sci. 64 (1) (2009) 59–68.
[84] C. Wang, H. Luo, X. Luo, H. Li, S. Dai, Equimolar CO 2 capture by imidazolium-based ionic liquids and superbase systems, Green Chem. 12 (11) (2010) 2019–2023.
[85] Z.-Z. Yang, L.-N. He, Y.-N. Zhao, B. Li, B. Yu, CO 2 capture and activation by superbase/polyethylene glycol and its subsequent conversion, Energy Environ. Sci. 4 (10) (2011) 3971–3975.
[86] C.-H. Yu, C.-H. Huang, C.-S. Tan, A review of CO2 capture by absorption and adsorption, Aerosol Air Qual. Res. 12 (5) (2012) 745–769.
[87] E. Kuram, B. Ozcelik, Multi-objective optimization using Taguchi based grey relational analysis for micro-milling of Al 7075 material with ball nose end mill, Measurement 46 (6) (2013) 1849–1864.
[88] G. Rochelle, E. Chen, S. Freeman, D. Van Wagener, Xu Q., A. Voice, Aqueous piperazine as the new standard for CO2 capture technology, Chemical engineering journal 171 (3) (2011) 725–733.